[Tech : Journal of Engineering Science](https://jurnal.sinesia.id/index.php/tech/index)
Vol. 2, No. 1, 2026.
e-ISSN: 3109-7790 (online)
https://jurnal.sinesia.id/index.php/tech/index

Multiscale Characterization of Two-Phase Flow in Coal Using CT Imaging and Simulation

Multiscale Characterization of Two-Phase Flow in Coal Using CT Imaging and Simulation

Sindi Parashayu Anugerah
E-mail Korespondensi : Sindianugerah25@gmail.com
School of Safety Science and Engineering, Shandong University of Science and Technology, P.R China

Info Article
| Submitted: 12 April 2026 **| Revised**: 15 May 2026 **| Accepted**: 23 May 2026
| Published: 23 May 2026
How to Cite : Sindi Parashayu Anugerah, "Multiscale Characterization of Two-Phase Flow in Coal Using CT Imaging and Simulation", *Tech : Journal of Engineering Scince*, Vol. 2, No. 1, 2026, P. 132-150.

ABSTRACT

Coal is a porous medium with strong heterogeneity, and its pore fracture structure plays a critical role in governing fluid flow behavior relevant to coalbed methane extraction and subsurface fluid management. However, accurate characterization of this structure has been challenging due to the limitations of conventional experimental methods. In this study, high resolution X-ray computed tomography was used to investigate the pore fracture structure of coal and its influence on gas water two-phase flow behavior. Six coal samples with different degrees of metamorphism were scanned, and three-dimensional digital models were reconstructed after image denoising, segmentation, and representative volume selection. Quantitative characterization of pore structure was performed by analyzing parameters such as pore size distribution, porosity, coordination number, and throat length. Pore network models were then extracted to simulate both single-phase and two-phase flow processes. The results showed that gas displacement by water followed a non-piston like mechanism, with preferential flow through connected pathways and gas trapping in isolated pores due to capillary effects. Relative permeability exhibited strong saturation dependence and hysteresis behavior, which were closely related to pore structure heterogeneity and connectivity. These findings provided important insights into the relationship between coal microstructure and fluid displacement efficiency, offering theoretical support for improving coalbed methane recovery.

Keywords: *CT Technology, Pore Fracture Characterization, Pore Network Modelling, Three-Dimentional Reconstruction, Two-Phase Flow*

Introduction

Coal remains a cornerstone of the global energy system and continues to dominate the energy structure in China due to its abundant reserves, mature extraction technologies, and stable supply capacity. Despite the rapid growth of renewable energy, coal is expected to play a sustained role in ensuring energy security and supporting industrial development. Consequently, improving the efficiency, safety, and environmental performance of coal utilization has become a critical scientific and engineering priority.

Coal seam gas, primarily methane, represents both a valuable clean energy resource and a major safety concern in underground mining. Its effective extraction simultaneously mitigates greenhouse gas emissions and reduces the risk of gas related hazards. In China, coal seam gas is increasingly recognized as a strategic unconventional resource, and its efficient development relies on a multiscale understanding of coal reservoir properties (Moore, 2012). However, large scale extraction remains challenging due to the intrinsically low permeability and pronounced heterogeneity of coal seams. At the core of these challenges lies the pore fracture system, which governs gas storage and transport within the coal matrix. The spatial distribution, connectivity, and geometric complexity of pores and fractures directly control permeability and fluid migration behavior. Enhancing permeability is therefore a key objective in coal seam gas recovery. Among available techniques, water injection has been widely adopted as an effective approach to improve permeability and operational safety. It has been shown to suppress coal dust, prevent gas explosions, and alleviate rock burst risks (Lu et al., 2017), while also promoting gas desorption and migration by increasing pore pressure and reducing capillary resistance (Karacan et al., 2011).

A fundamental requirement for understanding and optimizing such processes is the accurate characterization of the pore–fracture structure. Existing methods can be broadly categorized into physical testing, microscopic observation, and three-dimensional (3D) reconstruction approaches (Liu et al., 2020; Yao et al., 2009). Physical testing techniques, including mercury intrusion porosimetry and low-pressure nitrogen adsorption, provide quantitative information on pore size distribution and surface area but are inherently indirect and may disturb the native structure under high pressure conditions (Fu et al., 2021; Rigby, 2025; Schlumberger & Thommes, 2021). Microscopic observation methods, such as scanning electron microscopy, offer high-resolution imaging of surface features but are restricted to two-dimensional representations and lack the ability to capture internal connectivity (Wildenschild & Sheppard, 2013). Recent advances in X-ray based techniques have enabled non-destructive, three-dimensional characterization of coal microstructures. In particular, X-ray computed tomography has emerged as a powerful tool for resolving pore fracture networks and quantifying their geometric attributes (Blunt, 2017). Through image processing workflows involving denoising, segmentation, and reconstruction, key structural descriptors including porosity, pore size distribution, coordination number, and tortuosity can be extracted (Wang et al., 2023). Nevertheless, the limited resolution of computed tomography restricts its ability to resolve nano-pores, necessitating the integration of complementary techniques for multiscale characterization (Sakhaee-Pour & Bryant, 2012; Zou & Yang, 2012).

Previous studies have demonstrated that pore structure heterogeneity, including variations in size distribution, connectivity, and fractal characteristics, exerts a strong control on fluid flow behavior and permeability evolution in coal (Cai et al., 2013; Dantas et al., 2019; Y. Li et al., 2019; Z. Li et al., 2019; Wen et al., 2021; S. Zhang et al., 2019; Zhao et al., 2024). Such heterogeneity gives rise to complex displacement mechanisms, including preferential flow, phase interference, and capillary trapping, which cannot be adequately described by conventional continuum-scale models (Zheng et al., 2020; Zhou et al., 2021). This highlights the need for pore-scale approaches that explicitly incorporate realistic microstructural information.

In this research, the present study develops an integrated framework combining high-resolution X-ray computed tomography, three-dimensional reconstruction, and pore network modeling to investigate gas–water two-phase flow behavior in coal. Digital coal models were constructed from CT images and quantitatively characterized, followed by pore network extraction to simulate single-phase and two-phase flow processes. The primary objective is to elucidate the relationship between pore structure heterogeneity and fluid displacement dynamics at the pore scale, thereby providing mechanistic insights and theoretical guidance for enhancing coal seam gas recovery.

Research Methods

CT scanning was employed to characterize the internal microstructure of coal samples, including pores and fractures that govern fluid transport pathways. The acquired structural information was subsequently used as the basis for pore-scale numerical simulation to investigate gas water two-phase flow behavior. This integrated approach enabled quantitative evaluation of pore connectivity, permeability, and fluid displacement efficiency, providing a foundation for optimizing gas extraction processes and improving safety in coal mining operations.

Coal samples were first subjected to X-ray computed tomography scanning to obtain high-resolution three-dimensional images of their internal structure. The raw CT images were processed using image processing software (**Avizo, Thermo Fisher Scientific, Waltham, MA, USA**). Median filtering was applied to reduce noise while preserving edge features, and threshold-based segmentation was performed to distinguish pore–fracture regions from the coal matrix. Representative elementary volumes were then selected based on porosity convergence criteria, and three-dimensional digital models were reconstructed for further analysis. Quantitative characterization of the reconstructed pore–fracture structure was conducted by extracting key structural parameters, including porosity, pore size distribution, coordination number, and throat length. The connectivity and spatial distribution of pores were analyzed to evaluate heterogeneity within the coal samples. Volume rendering and visualization techniques were applied to examine the geometric features of the pore network and identify dominant flow pathways.

Following structural characterization, two-phase flow simulations were performed using **Dragonfly (Object Research Systems, Montreal, Canada)**. The reconstructed three-dimensional models were used as input to simulate water injection displacing gas within the pore–fracture network. The simulation incorporated fluid properties, boundary conditions, and interaction mechanisms to replicate realistic seepage behavior. Key parameters, including fluid saturation distribution, permeability, and flow velocity, were calculated to evaluate gas displacement efficiency under different injection conditions.

This combined experimental and numerical methodology enabled a detailed investigation of gas–water interaction at the pore scale. The results provided insights into displacement mechanisms, including preferential flow and gas trapping, and demonstrated the effectiveness of water injection in enhancing gas recovery while reducing the risk of gas accumulation in coal seams.

2.1 Coal sample preparation and selection

Coal samples used in this study were collected from the Songjiagou Coal Mine in Xunyi County, Shaanxi Province; the Bayangaole Coal Mine in Inner Mongolia; the Caozhuang Coal Mine of Shandong Feikuang Group; the Dahuangshan Coal Mine in Jinta, Xinjiang. The coal samples used in the CT experiments were cut from a large block of coal and then drilled into cylindrical shapes using a specially designed small sized core drill bit. This is because the process of preparing the coal samples inevitably creates sharp edges, which can cause edge enhancement during CT scanning.

2.2 Image noise reduction

Although CT images reflect coal pore–fracture structures, they are limited to two-dimensional slices. Three-dimensional reconstruction enables a comprehensive view of internal pore networks (Flannery et al., 1987). However, CT images often contain noise that can distort structural details, and reconstructing all slices is computationally intensive. Preprocessing is therefore required to enhance accuracy.

Common filtering techniques include Gaussian, mean, and median filtering (Ahmed & Islam, 2018; Pollnow et al., 2018; X. Zhang & Zhang, 2016). Gaussian filtering reduces normally distributed noise, and mean filtering smooths image noise, but both may blur edges and fine features. Median filtering, a nonlinear method, replaces each pixel with the median of its neighborhood, effectively removing noise while preserving edges and structural details.

Application of median filtering significantly improved image clarity and contrast, facilitating threshold segmentation and accurate three-dimensional reconstruction of coal pore fracture networks, as shown in Figure 2.

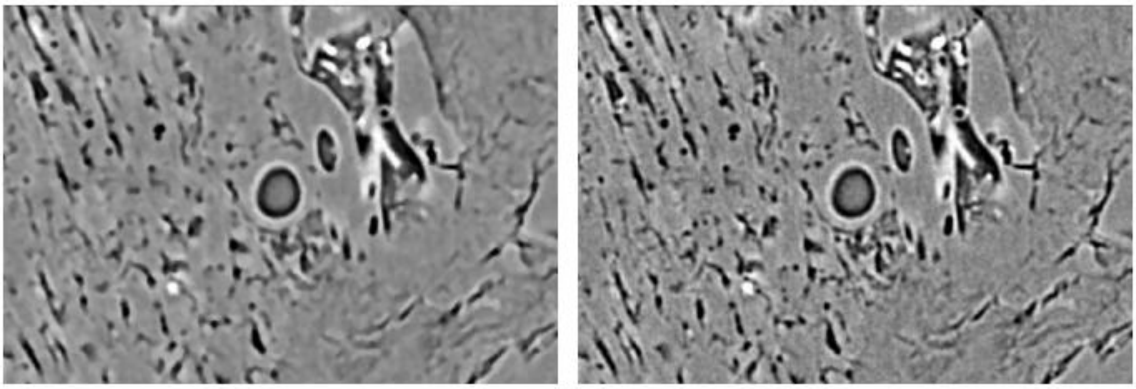

Fig.2 CT picture noise reduction

2.3 CT 3D reconstruction

Two-dimensional CT images provide preliminary information on the pore and fracture structure of a single cross section but cannot capture the full internal structure or quantitatively extract microscopic parameters such as pore number, diameter, or volume for the entire coal sample. To address this, the pore and fracture structure must be reconstructed in three dimensions for intuitive visualization and quantitative analysis of microscopic parameters (Zheng et al., 2020). The processed images and unit volume calculations are imported into **AVIZO** for 3D reconstruction using the **Generate Surface** module, which employs the **Marching Cubes** algorithm. This method analyzes cube voxels slice by slice, extracting materials of interest and connecting them into triangular facets to form a continuous 3D structure, known as **isosurface extraction**.

2.4 Two Phase Flow Simulation of Coal Based on CT 3D Reconstuction

Pore network models (PNMs) for four representative sub-volumes (S1–S4) were extracted from segmented 3D micro-CT images using a workflow in **Dragonfly** with **OpenPNM**. Segmentation converted raw grayscale data into a binary representation, distinguishing voids from the solid matrix. Grayscale thresholding was applied empirically for each sub-volume based on histogram analysis and pore morphology, ensuring the segmented pore space accurately reflected the true porous structure. Although empirical, this approach is widely used in micro-CT analysis and significantly affects quantitative pore characteristics and connectivity, highlighting the importance of careful threshold selection for accurate PNM construction (Gostick et al., 2016).

Results and discussion

1.1 Establishment of centerline model and pore network analysis

A centerline model was constructed from high-resolution CT images to quantitatively characterize coal pore structures and establish realistic pore networks. Image preprocessing preserved pore morphology while minimizing noise, and adaptive threshold segmentation distinguished pores from the coal matrix using locally optimized thresholds. Segmentation produced binary images representing the spatial distribution of pores. Individual pores were labeled and analyzed for geometric parameters (area, perimeter, equivalent radius, centroid), with morphological operations removing isolated pixels and repairing minor discontinuities to ensure accurate porosity and connectivity assessment.

Pore connectivity was determined by identifying throats the narrowest links between adjacent pores using the distance transform method. Pores and throats were represented as nodes and edges in a network, with coordination numbers indicating the degree of connectivity. Centerlines connecting pore centroids through throats formed a skeletonized network that maintained the original topology while enabling quantitative analysis of coordination, throat length, and connectivity ratios. Model parameters, including porosity, pore size, and specific surface area, were consistent with conventional measurements, validating the reconstruction workflow.

Table 3.1 Heterogeneity of the parameters of four coal samples.

Parameters		S1	S2	S3	S4
Porosity (%)	Pores	52	51.07	50.94	50.71
	Fractures	48	48.92	49.05	49.29
Direction proportion (%)	0°~30°	43.7	46.47	71.96	24.52
	30°~60°	19.8	20.5	15.87	23.50
	60°~90°	36.4	33.03	12.18	52.05
Volume proportion (%)	Connected pores	26.5	40.62	47.36	40.34
	Isolated pores	73.4	59.37	52.63	59.65

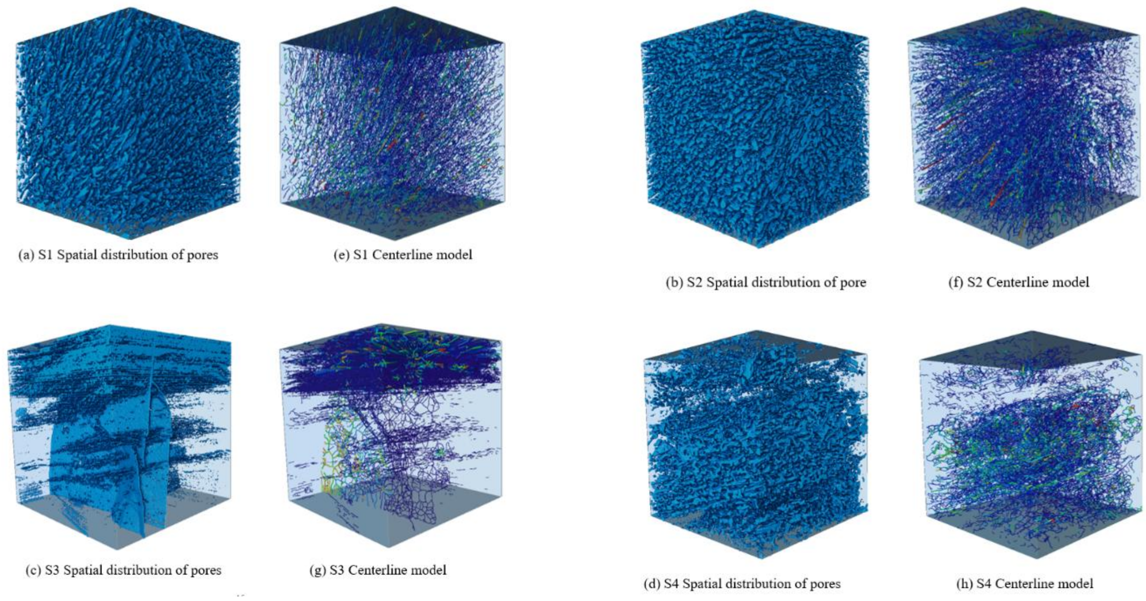

Fig. 3. (a)-(d) Spatial distributions of pores/fractures in S1, S2, S3 and S4 (e)-(h) their centerline models

Analysis of samples S1–S4 revealed significant structural heterogeneity. Pore content ranged from 50.71% to 52.0%, and fracture content from 48.0% to 49.29%, indicating both pores and fractures contribute to fluid storage and transport. Directional analysis showed anisotropy: S3 exhibited a dominant 0°–30° orientation (71.96%), while S4 was oriented mainly at 60°–90° (52.05%). S1 and S2 were more isotropic, suggesting that fluid flow is highly direction-dependent.

Connectivity varied among samples: S1 had the lowest connected pore proportion (26.5%), reflecting limited flow pathways, whereas S3 had the highest connectivity (47.36%), indicating a well-interconnected network. S2 and S4 were intermediate (>40%). These results highlight that connectivity, more than porosity alone, controls fluid transport efficiency.

Overall, the centerline model simplifies complex pore geometry while preserving key structural characteristics. Samples with higher connectivity and aligned pore orientations favor continuous preferential flow paths, enhancing gas-water displacement, whereas samples with isolated pores restrict flow. The findings demonstrate that coal pore-fracture structure particularly connectivity and anisotropy dominates fluid migration behavior, providing a robust foundation for pore-scale two-phase flow simulations.

1.2 Pore/fracture tortuosity characteristic

Microstructural analysis in Figure 3 reveals clear relationships between pore geometry and fluid transport. Smaller pores and shorter chord lengths consistently exhibit higher tortuosity, forming winding, complex pathways, whereas larger pores show lower tortuosity, creating more direct flow channels.

This pattern has significant implications for fluid movement. Highly tortuous micro-pores increase flow resistance due to longer pathways and greater friction, acting primarily as storage zones with limited contribution to advective transport. In contrast, larger, less tortuous pores serve as dominant conduits, facilitating efficient fluid migration. Consequently, effective hydraulic conductivity depends not only on total porosity but also on pore size distribution and geometric complexity.

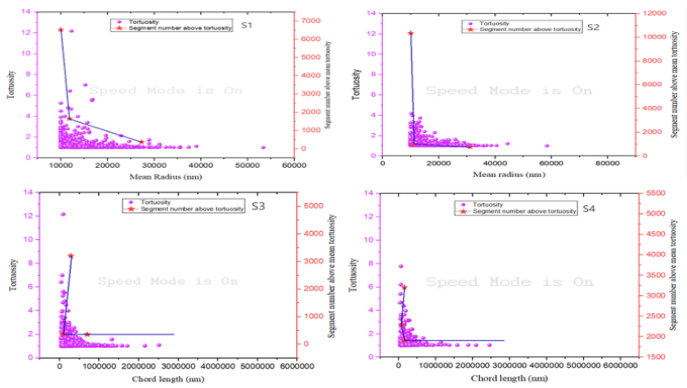

Fig. 3.2. (a)-(b) Relationships between average radius and (c)-(d) chord length with tortuosity

The correlation between small pore size and high tortuosity underscores the importance of microstructural characteristics in controlling macroscopic transport properties. Models based solely on porosity may overlook the influence of pore shape, connectivity, and pathway complexity, leading to inaccurate predictions. For multiphase flow in coal seams, such detailed structural insight is critical, as variations in pore architecture directly affect gas displacement by injected fluids and overall extraction efficiency. Incorporating parameters like pore size, tortuosity, and connectivity is therefore essential for accurate simulation and understanding of fluid migration in heterogeneous coal networks.

1.3 Relationship Between Pore Size and Shape Factor in Coal Samples

Morphological characterization of coal pore structures is essential for understanding storage and transport mechanisms, as the geometry of individual pores directly governs microscale fluid behavior. While total porosity provides a volumetric measure, it is the quantitative relationship between pore size and shape that dictates macroscopic properties such as permeability, compressibility, and surface availability for adsorption. This study systematically investigates pore size, shape factor, and surface area across four coal samples (S1–S4), representing a range of coal ranks and lithotypes, to establish predictive correlations that capture morphological heterogeneity.

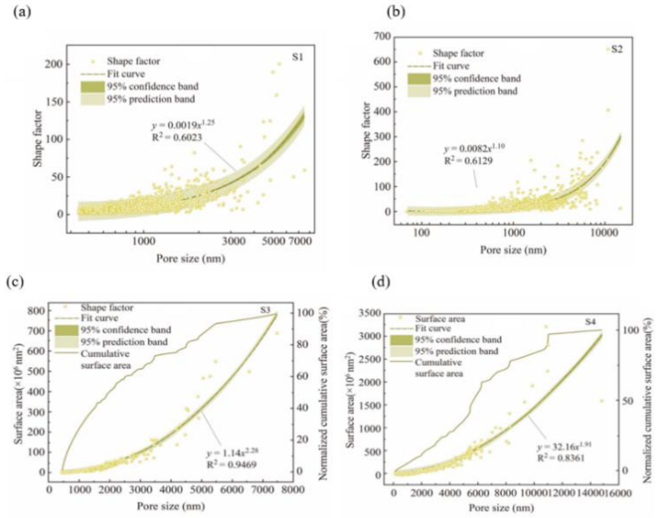

Figure 3.3. (a)-(b) Shape factor and (c)-(d) surface area distribution under different pore size range

The shape factor exhibits a strong exponential dependence on pore size, with curve fitting within the 95% confidence interval producing equations of $y = 0.0019x^{1.25}$ and $y = 0.0082x^{1.10}$ for samples S2 and S3, respectively. This trend indicates that larger pores have a higher tendency to propagate outward, resulting in increased shape factors and more complex surface geometries. In contrast, the correlation for sample S1 is less pronounced, which can be attributed to its limited population of pores and fractures, highlighting the influence of pore abundance on statistical fitting. When examining pore surface area as a function of pore size, even stronger exponential relationships emerge. The fitting results for samples S1, S2, and S3 $y = 21.93x^{1.91}$, $y = 1.14x^{2.28}$, and $y = 32.16x^{1.91}$, respectively demonstrate notable differences in how surface area scales with pore growth across the samples.

1.4 Relationship Between Pore Size and Shape Factor in Coal Samples

Pore network models (PNMs) for four sub-volumes (S1–S4) were extracted from 3D micro-CT images using **OpenPNM** in **Dragonfly**. Segmentation converted grayscale data into binary images, distinguishing pores from the solid matrix. Threshold values were chosen empirically for each sub-volume based on histogram analysis and pore morphology to ensure accurate representation of the pore space.

Although empirical, this approach is commonly used in micro-CT studies and critically affects pore geometry, size distribution, and connectivity measurements. Careful threshold selection ensures reliable PNM construction, providing a robust basis for quantifying structural heterogeneity and informing subsequent analyses of fluid transport, permeability, and seepage behavior in coal samples.

Table 3.4 summarizes the segmentation parameters used for each sub-volume such as threshold intensity ranges and voxel resolutions as well as the calculated absolute permeability values derived from the corresponding pore network simulations. The comparative analysis of these parameters across sub-volumes provides insight into how microstructural heterogeneity and pore geometry influence bulk transport properties, a fundamental consideration in interpreting pore-scale imaging data and in the development of predictive models for reservoir characterization.

Table 3.4 Segmentation parameters and absolute permeability results

Sample	Segmentation Range (Min–Max)	Pore Structure Characteristic	Absolute Permeability (mm^2)
S1	130 – 250	Density based distribution with multiple peaks	25,666.00
S2	34 – 250	Density based distribution similar to S1	25,666.00
S3	188 – 252	Connectivity based distribution²	25,606.60
S4	188 – 252	Connectivity based distribution	25,606.60

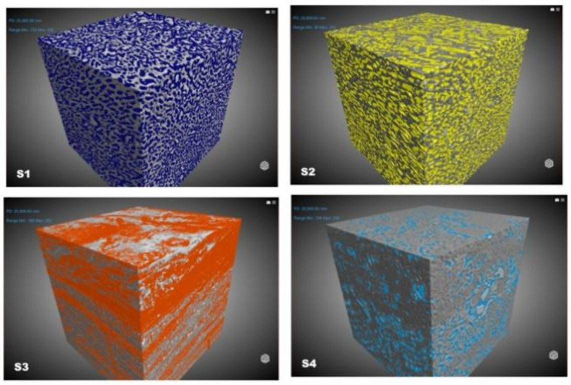

Fig. 3.4. (a) Segmented 3D Reconstructions of Pore Geometry

Several important insights emerge from this analysis. **S1** represents the baseline μCT reconstruction, capturing the complete, intricate pore network in gray, including both micro- and macropores. **S2**, **S3**, and **S4** employ a sphere-based Pore Network Modeling (PNM) approach, simplifying the void space into discrete pore bodies to facilitate detailed evaluation of pore size, spatial distribution, and connectivity. Across these models, a systematic trend is observed: from S2 to S4, average pore size increases while pore density and overall connectivity decrease. S2 features densely packed, small, highly connected pores, whereas S4 contains larger, more isolated voids with lower connectivity.

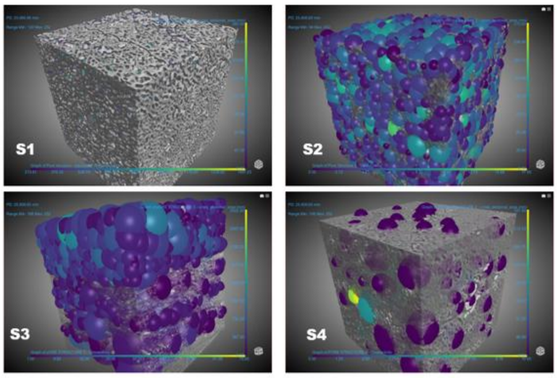

Fig. 3.4. (b) Pore Network Topology and Connectivity Distributions

The consistent permeability observed for S1 and S2, despite markedly different segmentation thresholds, validates the robustness of the extraction workflow. Permeability simulations are not highly sensitive to the precise threshold, provided that the percolating backbone is preserved. The similarity between S3 and S4, despite differences in cross-sectional pore areas, indicates that network connectivity rather than absolute pore size primarily governs flow. S4's smaller pores achieve comparable permeability to S3's larger pores, suggesting more efficient flow paths or higher connectivity. Slightly lower permeability in S3 and S4 compared to S1 and S2 likely reflects the exclusion of minor flow pathways through more restrictive thresholds. Overall, bulk permeability varies by less than 0.25%, confirming the representativeness of the sub-volumes. Among the sphere-based PNMs, S3 stands out as the optimal model for two-phase flow simulations. Its combination of substantial connectivity and heterogeneous pore size distribution captures primary flow pathways while retaining smaller pores that contribute to capillary trapping and phase interference. Color-coded connectivity in S3, reaching up to 70, emphasizes a well-integrated network that balances computational efficiency and physical fidelity. High-resolution µCT imaging combined with PNM enables quantitative analysis of the three-dimensional pore-throat architecture, linking microstructural geometry to observed permeability trends. These models reveal how pore connectivity, size distribution, and spatial arrangement govern macroscopic transport behavior, providing a robust basis for selecting representative digital cores. S3, in particular, offers a reliable digital model for simulating fluid displacement, accurately reflecting the complex interplay of pore-scale structure, connectivity, and two-phase flow dynamics in coal matrices.

1.5 Two-Phase Flow Characteristics During Fluid Displacement

The movement and distribution of water and gas within coal pore networks are key factors controlling coalbed methane (CBM) recovery. In coal seams, the wetting phase (water) displaces the non-wetting phase (methane), and the efficiency of this process depends on pore geometry, connectivity, capillary forces, and fluid properties. Coal's heterogeneous structure, including multiscale pores, micro-fractures, and cleat systems, produces complex flow patterns such as preferential channels, bypassing, and residual phase trapping. Consequently, displacement efficiency is governed not only by fluid properties but also by pore size distribution, tortuosity, and network connectivity (Bear, 2013; Clarkson & Bustin, 1999; Mohanty, 1992).

Advances in X-ray computed tomography (CT) allow high-resolution reconstruction of digital coal cores, enabling quantitative visualization of pore structure, connectivity, and spatial heterogeneity. When combined with computational fluid dynamics or pore network modeling, these digital cores can simulate two-phase flow, capturing dynamic saturation evolution, phase distribution, and preferential flow pathways (Andrew et al., 2014; Blunt, 2017; Wildenschild & Sheppard, 2013).

In this study, two-phase flow during water injection into gas-saturated coal is systematically investigated using CT-derived digital cores. Absolute and relative permeability, pore connectivity, and microstructural heterogeneity are analyzed to understand their influence on fluid displacement. Sample S3 is selected as a representative model, as its combination of high connectivity and heterogeneous pore sizes captures primary flow paths while retaining smaller pores for capillary trapping. This approach links pore-scale features to macroscopic transport behavior, providing insights into the mechanisms controlling water-gas displacement. The results support improved water-driven gas recovery and offer a framework for predicting multiphase flow in low-permeability coal reservoirs (Liao et al., 2025).

Table 3.5 Invading and Defending Phase Parameters for Sample 3.

Invader Value	Defender Value
0.7	0.92
0.8	0.96
0.9	0.99
1.0	1.00

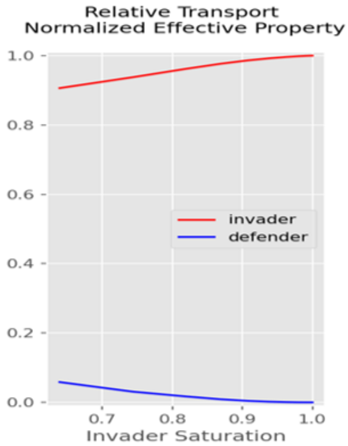

Fig. 3.5. Phase saturation evolution during two-phase displacement

The results for Sample 3, as presented in Fig.4.2.1, demonstrate a clear and progressive relationship between the invading phase and the defending phase during the displacement process. It should be noted that the values reported in the table do not strictly represent in-situ phase saturations, as their sum exceeds unity. Instead, these values are interpreted as normalized or simulation-derived parameters that describe the relative evolution of fluid distribution during two-phase flow. Such representation is commonly adopted in numerical simulations to illustrate trends in displacement behavior rather than exact physical saturation values. From the observed data, the increase in the invader values corresponds to the continuous injection of water into the pore space, while the defender values reflect the response of the gas phase during displacement. At the initial stage of the process, a relatively rapid increase in the defender-related values is observed, indicating that gas within the coal structure is effectively mobilized. This behavior suggests that the pore-fracture network in Sample 3 exhibits a relatively good degree of connectivity, allowing fluid to flow through preferential pathways with minimal resistance. As the displacement progresses, the rate of increase in the defender values gradually decreases, indicating a transition in flow behavior. This change can be attributed to the influence of capillary forces, pore-throat constrictions, and structural heterogeneity, which begin to restrict fluid movement. In this stage, part of the gas phase becomes increasingly difficult to displace, as it may be trapped in smaller pores or isolated regions within the coal matrix. This phenomenon reflects the non-uniform nature of coal pore structures and highlights the limitations of displacement efficiency under realistic conditions. At higher invader values, the system approaches a relatively stable state, where further water injection results in only minor changes in the defender phase. This indicates that most of the mobile gas has already been displaced, while the remaining gas is likely trapped due to capillary effects and poor connectivity. The displacement process therefore deviates from an ideal piston like mechanism and instead exhibits characteristics of heterogeneous two-phase flow, governed by pore scale structural complexity.

Overall, the results for Sample 3 illustrate that fluid displacement in coal is strongly controlled by microstructural features, including pore size distribution, connectivity, and fracture development. The observed trends highlight the importance of considering these factors when analyzing two-phase flow behavior, as they directly influence saturation evolution, flow pathways, and displacement efficiency. These findings provide valuable insights into the mechanisms of water driven gas migration in coal seams and contribute to a more accurate understanding of two-phase flow processes in low-permeability porous media.

Conclusion

This study presents a comprehensive investigation of coal pore-fracture structures and their influence on two-phase gas-water flow through the integration of high-resolution CT-based three-dimensional reconstruction, pore network modeling (PNM), and fractal analysis. Coal samples from multiple regions were analyzed, and optimal image preprocessing, including median filtering and empirically determined thresholding, enabled accurate segmentation and reliable reconstruction of pore networks. Representative elementary volumes of 500 voxels per side were established, and detailed 3D models generated in AVIZO captured key structural characteristics, including connectivity, pore size distribution, and tortuosity.

Quantitative analyses demonstrated that pore connectivity and tortuosity strongly govern fluid migration. Smaller or more tortuous pores impede flow, while larger, well-connected pores facilitate efficient transport. Centerline and PNM analyses provided a simplified yet representative framework for evaluating flow pathways, while fractal analysis. quantified structural complexity, revealing that volumetric fractal dimensions negatively correlate with porosity and permeability, and tortuosity fractal dimensions significantly influence fluid mobility.

Two-phase flow simulations based on extracted pore networks highlighted the critical role of pore geometry and connectivity in gas-water displacement. Poorly connected or highly tortuous regions exhibited lower relative permeability and slower fluid displacement, whereas well-connected networks allowed more efficient gas extraction. Simulation results, validated against experimental measurements such as mercury intrusion porosimetry, confirmed the reliability of CT derived networks in predicting flow behavior.

Overall, the integrated methodology provides a robust, non-destructive approach to linking coal microstructure with multiphase flow dynamics. The insights gained enhance the understanding of gas-water interactions in coal seams and offer practical guidance for optimizing coalbed methane recovery and predicting fluid migration in heterogeneous porous media.

This study establishes a foundation for linking pore-scale structure to macroscopic flow, providing both theoretical and practical insights for improved resource recovery in low-permeability coal reservoirs

Suggestion

The main innovative points of the paper are as follows:

1. High-resolution CT scanning together with pore network modeling to create 3D coal pore-fracture structures. The system enables researchers to visually inspect and measure intricate pore networks without damaging materials which leads to better coal microstructure analysis than traditional research techniques.
2. The research employed two measurement techniques to assess coal pore network complexity through volumetric measurements and tortuosity fractal dimensions which the researchers found to influence both permeability and two-phase flow. The new method establishes a quantifiable connection between microstructure changes and fluid movement which enables scientists to study how pore shapes impact gas and water movement.
3. Two-Phase Flow Simulation Based on CT 3D Reconstruction: The study applied CT-derived pore networks to simulate gas water two-phase flow, enabling direct evaluation of fluid saturation distribution, relative permeability, and flow heterogeneity. This methodology allows more accurate predictions of multiphase flow in coal seams and provides a foundation for optimizing coalbed methane recovery strategies.

Acknowledgements

This work was supported by the National Natural Science Foundation of China (Nos. 52174194, 52274145 and 52404227).

Bibliography

Ahmed, S., & Islam, S. (2018). Median filter detection through streak area analysis. *Digital Investigation*, *26*, 100–106. https://doi.org/10.1016/j.diin.2018.08.002

Andrew, M., Bijeljic, B., & Blunt, M. J. (2014). Pore-scale imaging of trapped supercritical carbon dioxide in sandstones and carbonates. *International Journal of Greenhouse Gas Control*, *22*, 1–14. https://doi.org/10.1016/j.ijggc.2013.12.018

Bear, J. (2013). *Dynamics of fluids in porous media*. Courier Corporation.

Blunt, M. J. (2017). *Multiphase flow in permeable media: A pore-scale perspective*.

Cambridge university press.
Cai, Y., Liu, D., Pan, Z., Yao, Y., Li, J., & Qiu, Y. (2013). Pore structure and its impact on CH4 adsorption capacity and flow capability of bituminous and subbituminous coals from Northeast China. *Fuel*, *103*, 258–268. https://doi.org/10.1016/j.fuel.2012.06.055
Clarkson, C. R., & Bustin, R. M. (1999). The effect of pore structure and gas pressure upon the transport properties of coal: a laboratory and modeling study. 1. Isotherms and pore volume distributions. *Fuel*, *78*(11), 1333–1344. https://doi.org/10.1016/S0016-2361(99)00055-1
Dantas, S., Struckhoff, K. C., Thommes, M., & Neimark, A. V. (2019). Phase behavior and capillary condensation hysteresis of carbon dioxide in mesopores. *Langmuir*, *35*(35), 11291–11298. https://doi.org/10.1021/acs.langmuir.9b01748
Flannery, B. P., Deckman, H. W., Roberge, W. G., & D'Amico, K. L. (1987). Three-dimensional X-ray microtomography. *Science*, *237*(4821), 1439–1444. https://doi.org/10.1126/science.237.4821.1439
Fu, S., Fang, Q., Li, A., Li, Z., Han, J., Dang, X., & Han, W. (2021). Accurate characterization of full pore size distribution of tight sandstones by low-temperature nitrogen gas adsorption and high-pressure mercury intrusion combination method. *Energy Science & Engineering*, *9*(1), 80–100. https://doi.org/10.1002/ese3.817
Gostick, J., Aghighi, M., Hinebaugh, J., Tranter, T., Hoeh, M. A., Day, H., Spellacy, B., Sharqawy, M. H., Bazylak, A., & Burns, A. (2016). OpenPNM: a pore network modeling package. *Computing in Science & Engineering*, *18*(4), 60–74.
Karacan, C. Ö., Ruiz, F. A., Cotè, M., & Phipps, S. (2011). Coal mine methane: a review of capture and utilization practices with benefits to mining safety and to greenhouse gas reduction. *International Journal of Coal Geology*, *86*(2–3), 121–156. https://doi.org/10.1016/j.coal.2011.02.009
Li, Y., Zhang, Y., Zhang, L., & Hou, J. (2019). Characterization on pore structure of tectonic coals based on the method of mercury intrusion, carbon dioxide adsorption and nitrogen adsorption. *Journal of China Coal Society*, *44*(4), 188–1196. https://doi.org/10.13225/j.cnki.jccs.2018.1494
Li, Z., Liu, D., Cai, Y., Wang, Y., & Teng, J. (2019). Adsorption pore structure and its fractal characteristics of coals by N2 adsorption/desorption and FESEM image analyses. *Fuel*, *257*, 116031. https://doi.org/10.1016/j.fuel.2019.116031
Liao, W., Zhang, S., Lv, M., Zhao, Y., Yan, H., Shi, G., Nooraiepour, M., Ma, L., Spasennykh, M., & Song, Z. (2025). The impact of multi-cycle water invasion on underground gas storages and its controlling factors. *Frontiers in Earth Science*, *13*, 1650076. https://doi.org/10.3389/feart.2025.1650076

Liu, L., Cui, Z., Wang, J., Xia, Z., Duan, L., Yang, Y., Li, M., & Li, T. (2020). Pore size distribution characteristics of high rank coal with various grain sizes. *ACS Omega*, *5*(31), 19785–19795. https://doi.org/10.1021/acsomega.0c02569

Lu, Y., Ge, Z., Yang, F., Xia, B., & Tang, J. (2017). Progress on the hydraulic measures for grid slotting and fracking to enhance coal seam permeability. *International Journal of Mining Science and Technology*, *27*(5), 867–871. https://doi.org/10.1016/j.ijmst.2017.07.011

Maulidan, M. R., & Yuhertiana, I. (2024). *Kepatuhan PT . Giri Palma Dalam Memenuhi Wajib Pajak*. *3*(3).

Mohanty, K. K. (1992). *Porous media: Fluid transport and pore structure. By FAL Dullien, Academic Press, 574 pp., 1992*. Wiley Online Library. https://doi.org/10.1002/aic.690380819

Moore, T. A. (2012). Coalbed methane: A review. *International Journal of Coal Geology*, *101*, 36–81. https://doi.org/10.1016/j.coal.2012.05.011

Muhammad Alrizky Ekiawan. (2023). Pengelolaan Lingkungan Hidup dalam Norma Hukum Indonesia. *Jurnal Rechten: Riset Hukum Dan Hak Asasi Manusai*, *5*(2), 311. https://doi.org/10.29123/jy.v13i3.345

Pollnow, S., Pilia, N., Schwaderlapp, G., Loewe, A., Dössel, O., & Lenis, G. (2018). An adaptive spatio-temporal Gaussian filter for processing cardiac optical mapping data. *Computers in Biology and Medicine*, *102*, 267–277. https://doi.org/10.1016/j.compbiomed.2018.05.029

Rigby, S. P. (2025). Uses of gas sorption and mercury Porosimetry methods in studies of heritage materials. *Heritage*, *8*(4), 132. https://doi.org/10.3390/heritage8040132

Sakhaee-Pour, A., & Bryant, S. L. (2012). Gas permeability of shale. *SPE Reservoir Evaluation & Engineering*, *15*(04), 401–409. https://doi.org/10.2118/146944-PA

Saleh, M. (2022). Implementasi Pendidikan Karakter Di Sekolah Inklusi. *Hikmah: Journal of Islamic Studies*, *17*(2), 101. https://doi.org/10.47466/hikmah.v17i2.198

Schlumberger, C., & Thommes, M. (2021). Characterization of hierarchically ordered porous materials by physisorption and mercury porosimetry—a tutorial review. *Advanced Materials Interfaces*, *8*(4), 2002181. https://doi.org/10.1002/admi.202002181

Wang, S., Spurin, C., & Bultreys, T. (2023). Pore-scale imaging of multiphase flow fluctuations in continuum-scale samples. *Water Resources Research*, *59*(6), e2023WR034720. https://doi.org/10.1029/2023WR034720

Wen, Z., Wang, Q., Yang, Y., & Si, L. (2021). Pore structure characteristics and evolution law of different-rank coal samples. *Geofluids*, *2021*(1), 1505306. https://doi.org/10.1155/2021/1505306

Wildenschild, D., & Sheppard, A. P. (2013). X-ray imaging and analysis techniques for quantifying pore-scale structure and processes in subsurface porous medium systems. *Advances in Water Resources*, *51*, 217–246. https://doi.org/10.1016/j.advwatres.2012.07.018

Yao, Y., Liu, D., Che, Y., Tang, D., Tang, S., & Huang, W. (2009). Non-destructive characterization of coal samples from China using microfocus X-ray computed tomography. *International Journal of Coal Geology*, *80*(2), 113–123. https://doi.org/10.1016/j.fuel.2016.05.110

Zhang, S., Li, Y., & Qin, X. (2019). Pore fractal characteristic of coal reservoirs in Qinshui Basin and its influence on methane adsorption property. *Coal Science and Technology*, *47*(3), １６３ － １６７. https://doi.org/10.13199/j.cnki.cst.2019.03.024

Zhang, X., & Zhang, S. (2016). Diffusion scheme using mean filter and wavelet coefficient magnitude for image denoising. *AEU-International Journal of Electronics and Communications*, *70*(7), 944–952. https://doi.org/10.1016/j.aeue.2016.04.012

Zhao, W., Liu, H., Wang, H., Liu, D., & Li, X. (2024). Microscopic pore characteristics of coal seam and the controlling effect of sedimentary environment on pore structure in No. 8 coal seam of the Ordos Basin. *Coal Science and Technology*, *52*(6), 142–154. https://doi.org/10.12438/cst.2023-1112

Zheng, S., Yao, Y., Elsworth, D., Wang, B., & Liu, Y. (2020). A novel pore size classification method of coals: Investigation based on NMR relaxation. *Journal of Natural Gas Science and Engineering*, *81*, 103466. https://doi.org/10.1016/j.jngse.2020.103466

Zhou, H., Liu, Z., Sun, X., Ren, W., Zhong, J., Zhao, J., & Xue, D. (2021). The evolution characteristics of seepage channel during water infusion in deep coal samples. *Journal of China Coal Society*, *46*(3), 867–875.

Zou, C. Z. H. U., & Yang, Z. T. A. O. (2012). Types, characteristics, genesis and prospects of conventional and unconventional hydrocarbon accumulations: taking tight oil and tight gas in China as an instance. *Acta Petrolei Sinica*, *33*(2), 173. https://doi.org/10.7623/syxb201202001

Author Biographies

Sindi Parashayu Anugerah is a master's student in Safety Science and Engineering. Her research focuses on coal pore–fracture characterization using CT scanning technology and its influence on two-phase (gas–water) flow behavior. She applies advanced image processing and numerical simulation tools, such as AVIZO and Fluent, to analyze coal microstructure and seepage mechanisms. Her academic interests include energy resource engineering, digital rock physics, and subsurface fluid flow analysis.